Neutral Injection Requirements and Parameters for the ASDEX Tokamak

A. Stäbler

IPP 4/159 Juni 1977

MAX-PLANCK-INSTITUT FÜR PLASMAPHYSIK

8046 GARCHING BEI MÜNCHEN

MAX-PLANCK-INSTITUT FÜR PLASMAPHYSIK

GARCHING BEI MÜNCHEN

Neutral Injection Requirements and Parameters for the ASDEX Tokamak

A. Stäbler

IPP 4/159 Juni 1977

Die nachstehende Arbeit wurde im Rahmen des Vertrages zwischen dem Max-Planck-Institut für Plasmaphysik und der Europäischen Atomgemeinschaft über die Zusammenarbeit auf dem Gebiete der Plasmaphysik durchgeführt.

IPP 4/159

Neutral Injection Requirements and Parameters for the ASDEX Tokamak.

A. Stäbler

June 1977

Abstract

Neutral injection is planned as an additional heating method for the ASDEX tokamak. The required input power and the appropriate extraction voltage are determined by evaluating the beam penetration, the heating efficiency, the impurity increase associated with neutral injection and the net particle current added to the plasma. The calculations deal with the following items: beam absorption and fast ion confinement, radial particle deposition, slowing-down on plasma ions and electrons, losses due to charge exchange during beam trapping and fast ion slowing-down and (in a rather simplified way) the presence of a loss region. As a result of these calculations the following design parameters are proposed: extracted ion current: 4 x 40 A, extraction voltage: 40 - 50 kV, pulse length: 0.2 - 1.0 s. Assuming reasonable values for an ASDEX plasma, this will yield the following performance: power transferred to the plasma: $\simeq$ 2.5 MW, power to the ions: $\simeq$ 1.5 MW, impurity increase: $\Delta Z_{eff} \simeq$ 1.0 - 1.5 and particle refuelling: > 35 A. Furthermore, the possibility of varying the heating power profiles by changing the injection geometry is investigated.

C O N T E N T S

I. INTRODUCTION

Injection of fast neutral atoms is planned as additional heating method for the ASDEX tokamak, which is now under construction at IPP Garching /1/. Additional heating power is expected to allow the following objectives /2/:

- to study the collisionless regime for the plasma ions,
- to raise the upper limit for the attainable plasma density,
- to investigate the possibility of controlling temperature and current profiles.

The first two points call for an additional power absorbed in the plasma which lies well above the ohmic heating power (P_{OH} : 0.5 - 1.0 MW); the third point requires that this power can be radially deposited in a controlled manner.

In preparing the injection experiment on ASDEX, calculations were performed which should result in establishing the requirements to be met by the injection system, i.e. they should answer the following questions:

- How do the power delivered to the plasma and the radial power deposition depend on the injection parameters, and how much of this power is transferred to the ions and electrons?
- How many particles are added to the plasma by neutral injection?
- What is the impurity increase directly associated with the injection of fast atoms?

The report starts by treating absorption of the neutral beam (Section II). This includes total beam absorption as well as radial deposition of the fast ions. In the next section particle and energy losses due to charge exchange and scattering on non-confined orbits during the slowing-down

process are described (Section III). The impurity influx associated with neutral injection is considered in Section IV. On the basis of these more general considerations, calculations were performed assuming given values for the plasma and the injection system, leading to the determination of the parameters which should be aimed at for the injection experiment on ASDEX (Section V). The possibility of varying the heating power profiles for electrons and ions by changing the injection geometry is discussed in Section VI. A summary of the results including the shortcomings of the present considerations is given in the last section.

II. NEUTRAL BEAM ABSORPTION

The number of fast ions created per cm^3 and s by neutral injection, i.e. the local fast ion birth rate, can be written as follows /3/:

$$\dot{n}_f(r) = \frac{(I_o/e)}{2\pi R_o \pi a^2} H(r), \qquad \text{(II.1)}$$

where (I_o/e) is the particle current injected into the torus and H(r) is a (dimensionless) radial shape factor, also called "deposition profile", which may be calculated from the injection geometry, the particle energy and the various plasma parameters. Owing to its definition H(r) has to be normalized in the following way ($V_{pl} = 2\pi R_o \pi a^2$):

$$F \equiv (1/V_{pl}) \int_{V_{pl}} H(r)\, dV = (2/a^2) \int_o^a H(r)\, r\, dr, \qquad \text{(II.2)}$$

where F denotes the relative fraction of the neutral beam being absorbed and confined within the plasma.

The design of ASDEX enables beam injection tangential to the toroidal field. The calculations of H(r) were done in accordance with the work of Rome et al. /3/ and have been reported earlier /2/. Here, only the essential assumptions and results will be reviewed.

The injection geometry is sketched in fig. 1. For tangential injection, the fast ion orbits are, in good approximation, concentric circles about the stagnation point /3, 4/ displaced about $x_s \simeq \rho_{pol}$ (a/R) relative to the magnetic axis (ρ_{pol}: gyroradius in the poloidal field; co-injection: outward displacement; counter-injection: inward displacement). Particles born on orbits which intersect the plasma boundary are considered as lost. The fast ion birth rate is calculated, first as a function of the distance to the stagnation point, and then transformed into a function of r by averaging over the angle Θ.

Concerning the plasma, it is assumed: (1) the electron density is parabolic: $n_e(r) = n_e(0)*(1-(r/a)^2)$, (2) there is only one dominant impurity with charge number Z, (3) the effective charge number exhibits no radial dependence: $Z_{eff}(r) = \text{const.}$

With fixed injection geometry the only free parameter which determines the deposition profiles is a/λ_o, where λ_o is the absorption length at peak density $n_e(0)$. Beam absorption is due to the following processes (H^o injection into a hydrogen plasma): charge exchange on protons (σ_{cx}), ionization by electron impact (σ_{ie}), by proton impact (σ_{ii}) and by collisions with the impurity ions ($\sigma_I = Z^2\sigma_{ii}/5/$). This leads to the following total absorption cross-section:

$$\sigma_T(E_o) = \frac{Z - Z_{eff}}{Z - 1}\,\sigma_{cx}(E_o) + Z_{eff}\,\sigma_{ii}(E_o) + \frac{\langle\sigma v\rangle_{ie}(E_o)}{v_o} . \qquad \text{(II.3)}$$

The temperature dependence of the individual cross-sections does not greatly affect the total cross-section; temperature profiles have therefore been neglected. The function $\lambda_o(E_o) = 1/(\sigma_T*n_e(0))$ is plotted in fig. 2 for several values of $n_e(0)$ with Z_{eff} as parameter, assuming that eightfold charged oxygen (Z = 8) is the major impurity contribution. This assumption is kept throughout this study. Cross-sections and rate coefficients were taken from ref. /6/.

Figure 3 gives some results for H(r). The different curves were obtained by varying a/λ_o and the distance of the beam axis from the torus centre (R_c).

The numbers in parentheses in fig. 3 indicate the total amount of the injected beam (and also of the injected power) which is absorbed and confined within the plasma (eq. (II.2)). The relative losses due to incomplete absorption and confinement

$$D(a/\lambda_o) = 1 - (2/a^2) \int_o^a H(r)\, r\, dr = 1 - F(a/\lambda_o) \qquad \text{(II.4)}$$

are given in fig. 4. The R_c value of 144 cm corresponds to the middle of R_o and R_o-a, the optimum condition for pencil beam absorption /3/.

The requirements made on an "effective" injection experiment, concerning beam absorption and fast ion deposition, can be stated as follows:

- More than 90 % of the injected beam should be absorbed and confined within the plasma.
- The deposition profiles should be peaked in the plasma centre.

According to the results outlined above these requirements mean:

$$0.5 \lesssim a/\lambda_o \lesssim 2.0.$$

Curves with a/λ_o = const are plotted in a ($n_e(0)$-E_o) diagram (fig. 5). The region between the a/λ_o = 0.5 and a/λ_o = 2.0 lines indicates the plasma densities and the corresponding injection energies for which the requirements, mentioned above, are fulfilled.

III. FAST ION SLOWING DOWN

III.1 CHARGE EXCHANGE AND ENERGY TRANFER TO THE PLASMA

The energy transfer from the fast ions to the plasma may be seriously affected by charge exchange (CX) processes between the hot ions and the background neutrals. The effects of this process have been treated in a separate report /7/. The basic ideas of the calculations given there are summarized in the following.

If an energy interval ΔE is considered, the losses of fast ions, passing ΔE, are given by

$$\Delta N(E) = (dN/dt) * (dt/dE) * \Delta E \qquad \text{(III.1)}$$

where dN/dt is the source rate of neutrals due to CX: $dN/dt = -N*n_o*\sigma_{cx}(v)*v$. The term $dt/dE = -(t_s/2E)*(1+(E_c/E)^{3/2})^{-1}$ is obtained from classical collisions theory, where t_s denotes the Spitzer slowing-down time and E_c is the "critical" energy where the rate of loss of energy to the ions equals that to the electrons /4/. The loss of fast ion energy ($W(E) = N(E)*E$), associated with the CX processes, is therefore obtained by

$$\Delta W_L(E) = E * \Delta N(E). \qquad \text{(III.2)}$$

Energy integration of (III.1) and (III.2) from E_o to T_i and normalization to the particles and energy injected during one neutral beam pulse yield formulae for the relative particles loss L_p and relative energy loss L_w. Numerical results for L_p and L_w as functions of (n_o/n_e) are shown in fig. 6. Here, the full energy dependence of the cross-section $\sigma_{cx}(v)$ ($\underline{H}^+ + H^o \rightarrow \underline{H}^o + H^+$), given by Riviere /8/, was taken into account.

The energy transfer to the plasma ions and electrons can be calculated in a similar way. The total variation in fast ion energy is given by

$$\Delta W(E) = \Delta W_{pl}(E) + \Delta W_L(E) = N(E)\ \Delta E + E\ (dN/dE)\ \Delta E \qquad \text{(III.3)}$$

where $\Delta W_L(E)$, the fraction lost owing to CX, is determined by eq. (III.2). $\Delta W_{pl}(E)$ is transferred to the plasma particles ($f_I(E)$, $f_e(E)$: energy partition to ions and electrons, respectively):

$$\Delta W_{pe}(E) = (f_I(E) + f_e(E))\,N(E)\ \Delta E$$

$$f_I(E) + f_e(E) = 1 \qquad \text{(III.4)}$$

Integration and normalization lead to terms for G_I and G_e, the relative amounts of the input energy to the plasma ions and electrons, respectively. Results of such calculations are displayed in fig. 7.

Figures 6 and 7 show that the CX losses as well as the energy transfer strongly depend on the values of T_e and (n_o/n_e). These quantities exhibit a considerable radial dependence in a real tokamak plasma. The calculations have therefore been extended, taking into account arbitrary profiles of T_e, (n_o/n_e) and the particle deposition $H(r)$. Doing this, the radial and integral behaviour of L_p, L_w, G_I and G_e can be obtained:

$$L_{p,w} = (2/a^2) \int_o^a H(r)\ L_{p,w}(r)\ r\ dr,$$

$$G_{I,e} = (2/a^2) \int_o^a H(r)\ G_{I,e}(r)\ r\ dr. \qquad \text{(III.5)}$$

Here $L_p(r)$, $L_w(r)$, $G_I(r)$ and $G_e(r)$ were determined, considering the local values of (n_o/n_e) and T_e. Details of these calculations can be obtained from ref. /7/. Specific applications are used in Section V.

III.2 SCATTERING INTO THE LOSS REGION

Measurements on ORMAK have shown that the fast ion losses due to pitch-angle scattering on non-confined orbits may exhibit a significant effect on the net power given to the

plasma /9/. This is especially true of counter injection. An "exact" determination of this loss mechanism requires a solution of the time dependent fast ion distribution function including CX and the loss region (see, for example, /10/). Such calculations have not been performed for the ASDEX case until now. Estimations concerning these losses will be obtained in a rather simplified manner.

The position of the loss regions in velocity space has been determined in two different ways. On the one hand, guiding--centre orbits for the fast ions were explicitly calculated according to the formula of Rome et al. /10/. On the other hand, the approximate solution, given by the same authors, has been used. Results of these calculations for ASDEX are illustrated in fig. 8. The parameter r_b indicates the radius of the fast ion creation point. Particles which have $(v_{\parallel}, v_{\perp})$ values above their corresponding r_b curve are lost, while those with $(v_{\parallel}, v_{\perp})$ values below this curve are confined. The plasma current assumed in fig. 8 is I = 500 kA, and the current profile is $j(r) = j_o(1-(r/a)^2)^3$. The approximate solution agrees quite well with the results obtained from the particle orbits, especially with regard to the vertex of the loss cone which determines the minimum energy for which particles may be lost.

From the results in fig. 8 two interesting points should be emphasized. (1) The distance in velocity space from the loss region to the initial position of the counter injected ions is considerably smaller than to the initial position of the co-injected ions. (2) As long as $E_o \lesssim 50$ keV, fast ions born at radii $r_b \lesssim 25$ cm should not be lost by pitch--angle scattering. This good confinement behaviour is due to the relatively high value of the plasma current since the minimum energy below which all particles with fixed r_b are confined is proportional to I^2 /10/.

If the plasma current and the current profile are fixed, there is a definite relation between a given ion energy E_o and the corresponding birth radius $r_b(E_o)$ so that all particles with energies $E < E_o$ and radii $r_b < r_b(E_o)$ are confined. Using this relation the fraction of the injected beam (beam energy E_o) which may "potentially" be scattered into the loss region, can be calculated as follows (see eq. II.2):

$$L_{LR}(E_o) = (2/a^2) \int_{r_b(E_o)}^{a} H(r)\ r\ dr. \qquad \text{(III.6)}$$

Here, it is assumed that the radial fast ion distribution H(r) is not changed by pitch-angle scattering, and that the ion birth radius r_b agrees with its mean radius, i.e. the shift of the drift surfaces relative to the magnetic axis is neglected.

Figure 9 shows results of $L_{LR}(r) = (2/a^2) \int_r^a H(r')\ r'\ dr'$ for several deposition profiles. In almost all cases displayed here, the beam fraction deposited between r = 25 cm and the plasma boundary (r = 40 cm) is less than 25 % of the total injected beam.

The "real" losses during particle slowing-down are determined by the relation τ_s/τ_{sc}, where τ_s is the slowing--down time and τ_{sc} the characteristic time for pitch-angle scattering. For the plasma parameters considered here, τ_s and τ_{sc} are of the same order of magnitude. In order to get a rough estimate of the losses due to the presence of a loss region it is further assumed that (1) the loss region does not affect co-injected particles and (2) half of the counter-injected particles deposited between $r_b(E_o)$ and a will be lost with half of their initial energy E_o. This rather simplified treatment may be justified by the fact that the presence of a loss region does not play as important a role for the ASDEX injection as for the injection into smaller tokamaks with lower plasma currents.

IV. IMPURITY INFLUX

IV.1 PROCESSES WHICH CONTRIBUTE TO THE IMPURITY INFLUX

Both neutral beam absorption and fast ion slowing-down are accompanied by a loss of particles which escape from the plasma, may reach the walls and, by sputtering, cause an influx of heavy impurity atoms to the plasma. These particle losses are due to the following processes:

(1) Incomplete beam absorption
(2) Beam absorption on non-confined orbits
(3) Beam absorption by charge exchange
(4) Charge exchange during particle slowing-down
(5) Pitch-angle scattering into the loss region.

In order to determine the resulting impurity influx it is assumed that (1) all particles lost hit the walls (i.e. reionization is neglected) and (2) all atoms created by sputtering enter the plasma. These assumptions, obviously, lead to an upper limit for the impurity influx, directly associated with neutral injection. The impurity increase resulting from the heated plasma will not be regarded in this connection. A rough estimation of neutral reionization within the plasma is considered in Section IV.2.

The relative losses due to incomplete absorption and confinement ($D(a/\lambda_o)$) are given in eq. (II.4) and fig. 4. Since all co-injected particles (for $R_c \gtrsim 144$ cm and $E_o \lesssim 50$ keV) are absorbed on confined orbits, the not absorbed (D_1) and the not confined (D_2) beam fraction may be written

$$D_1(a/\lambda_o) = D_{CO}(a/\lambda_o),$$

$$D_2(a/\lambda_o) = D_{COUNTER}(a/\lambda_o) - D_{CO}(a/\lambda_o).$$

The resulting impurity influxes (neutral particle current I_o) are then given by

$$I_{S1} = I_o * D_1(a/\lambda_o) * S(E_o), \qquad \text{(IV.1)}$$

$$I_{S2} = (I_o/2) * D_2(a/\lambda_o) * S(E_o) \qquad \text{(IV.2)}$$

where $S(E_o)$ denotes the sputtering coefficient at energy E_o.

The relative amount of neutral beam being absorbed by charge exchange can be seen from eq. (II.3):

$$W_{cx}(E_o) = \frac{Z - Z_{eff}}{Z - 1} \times \frac{\sigma_{cx}(E_o)}{\sigma_t(E_o)}. \qquad \text{(IV.3)}$$

$W_{cx}(E_o)$ is illustrated in fig. 10. For a clean plasma and low injection energies CX is the dominant absorption process. The impurity influx caused by this process may be written

$$I_{S3} = I_o * (1 - D_1(a/\lambda_o)) * W_{cx}(E_o) * S(T_i). \qquad \text{(IV.4)}$$

Since the escaping particles have plasma temperature, the sputtering coefficient must be taken at $E = T_i$. An ion temperature profile is neglected.

The impurity influx due to CX losses during the fast ion slowing-down may be obtained by multiplying the particle losses $\Delta N(E)$ in the energy interval ΔE(eq. III.1) by the sputtering coefficient $S(E)$ and subsequently integrating from E_o to the thermal energy T_i. Details of this procedure as well as allowance for arbitrary plasma and deposition profiles are treated in ref. /7/. The result can be expressed as follows:

$$I_{S4} = I_o * (2/a^2) \int_o^a H(r) * (I_{S4}(r)/I_o) \; r \, dr \qquad \text{(IV.5)}$$

where $I_{S4}(r)$ stands for the local energy integral over $\Delta N(E)*S(E)$, which is proportional to I_o /7/.

The impurity influx due to the presence of a loss region may be estimated in accordance with the assumptions stated at the end of Sec. III.2. If the power injected into the torus in the co-direction equals that injected in the counter-direction, one obtains (eq. III.6)

$$I_{S5} = (I_o/2) * S(E_o/2) * (2/a^2) \int_{r_b(E_o)}^{a} H_{COUNTER}(r)\, r\, dr \quad \text{(IV.6)}$$

Figure 11 shows the behaviour of the various components of the total impurity influx (I_S/I_o). The sputtering coefficients used for these and all further calculations are taken from ref. /11/ (hydrogen on stainless steel). The essential parameters are: T_i = 1 keV, $T_e(0)$ = 1.5 keV, Z_{eff} = 2, $n_e(0) = 6 * 10^{13}$ cm^{-3}, $n_o(0) = 1.6 * 10^8$ cm^{-3}, $n_o(a) \simeq 40 * n_o(0)$. Details of the T_e and (n_o/n_e) profiles will be described in the next section. The deposition profiles H(r) are calculated according to the energy dependent a/λ_o values. The dominant contributions to the total impurity influx are provided by charge exchange during slowing-down (I_{S4}) and beam absorption by charge exchange (I_{S3}). This is true also of other realistic plasma parameters.

IV.2 EFFECTS OF FINITE REIONIZATION PROBABILITY

For plasma densities $n_e \gtrsim 2 * 10^{13}$ cm^{-3}, the mean free path versus ionization (λ_i) of a plasma neutral created by charge exchange is of the order of the ASDEX plasma pinch diameter. Neglect of reionization therefore overestimates the particle losses and the resulting impurity influx connected with beam absorption by CX. Hence, a lower limit of the reionization probability was estimated using the following assumptions: (1) A neutral created by CX with an injected atom will have only a radial, but no toroidal component of velocity. (From geometrical considerations such a neutral will most probably fly perpendicularly to

the injection direction, i.e. for "ideal" tangential injection it will stay on a plane perpendicular to the plasma column). (2) the escape probability is determined only by ionization processes. (3) The plasma parameters n_e, $T_{i,e}$ and Z_{eff} are assumed to be constant over the cross--section. They therefore determine a λ_i value for all neutrals.

The first two assumptions underestimate the path lengths of the neutrals between their creation point and the plasma boundary and therefore lead to a lower limit for the reionization probability. This probability was calculated by averaging first over all allowed distances between a fixed creation point and the plasma boundary. In a second step, the average was taken over all possible creation points. This results in a "mean reionization probability" <RP> depending on n_e, $T_{e,i}$ and Z_{eff}. Some results are given in fig. 12. The impurity influx due to beam absorption by CX (I_{S3}; eq. IV.4) must therefore be reduced by a factor of (1 - <RP>) if neutral reionization within the plasma should be taken into account. This yielded the results in Section V.

A similar estimation has also been performed concerning the reionization of the fast neutrals created during slowing--down. Here, T_i was replaced by $E \simeq E_o/2$ corresponding approximately to the mean energy of these neutrals. Owing to their longer mean free paths, however, reionization always remains small (< 20 %).

V. RESULTS FOR FIXED PLASMA AND INJECTION PARAMETERS

V.1 CHOICE OF PLASMA AND INJECTION PARAMETERS

In this section the calculations concerning beam absorption and fast ion slowing-down will be summarized, assuming parameters and profiles expected for an ASDEX plasma and taking into account that a neutral hydrogen beam delivered by any injection system consists of three energy components (E_o, $E_o/2$, $E_o/3$). Quantitative results will be obtained for the "heating efficiency" (i.e. the relative amount of the injected power absorbed by the plasma), the "refuelling efficiency" (i.e. the relative amount of the injected particle current absorbed and thermalized within the plasma) and the impurity increase associated with neutral injection.

Concerning the "refuelling efficiency", some additional remarks have to be made. The particles lost by beam trapping due to CX and by CX processes during fast ion slowing-down contribute to the total particle losses. A lower limit for the reionization probability of the CX neutrals has been included, thus leading to an upper limit for particle and energy losses and for the impurity influx caused by these losses. Consequently, a lower limit will be obtained for the resulting "refuelling efficiency". Furthermore, charge exchange during fast ion slowing-down causes a neutral background particle to become a plasma ion with thermal energy. Concerning the plasma ion balance one may therefore argue that no particle loss has taken place. However, as long as the possibility of escaping from the plasma is much larger for the fast neutral created by CX than it is for the thermal neutral, this argument cannot be upheld since there is a great chance of the background neutral becoming a plasma ion, even without charge exchange

with the fast ion. In other words, CX of fast ions during slowing-down reduces the neutral density and therefore reduces the source term $n*n_o <\sigma_{ion} v>$ in the plasma ion balance equation. Nevertheless, the particle losses, as calculated here, result in a lower limit for the "refuelling efficiency" from this point of view, too. An upper limit, concerning this point, will be obtained by neglecting the contribution of CX during slowing-down in the following results.

The planned operating data of ASDEX are: R_o = 164 cm, a = 40 cm, B_t = 3 T and I_p = 0.5 MA /1/. Concerning the plasma, the following parameters are assumed: $T_e(0)$ = 1.5 keV, T_i = 1 keV, $n_e(0) = 3*10^{13}$ cm^{-3} and $6*10^{13}$ cm^{-3}, Z_{eff} = 2. A radial dependence is taken into account for T_e, n_e and (n_o/n_e). Parabolic density profiles $n_e(r) = n_e(0)*(1-(r/a)^2)$ ($\overline{n}_e = 0.5*n_e(0)$) were used for calculating the radial particle deposition, and T_e and (n_o/n_e) profiles were taken from a tentative run with a simulation code /12/. They are displayed in fig. 13. The absolute value of (n_o/n_e) in the plasma centre was adjusted to corresponding $n_o(0)$ values of about 10^8 cm^{-3} as measured in other tokamaks. For each of the two plasma densities assumed, calculations were performed with $(n_o/n_e)(0) = 1.3*10^{-6}$ and $(n_o/n_e)(0) = 2.6*10^{-6}$ leading to four different sets of plasma parameters which will be identified hereafter by the abbreviations:

P1: $n_e(0) = 3*10^{13}$ cm^{-3}, $(n_o/n_e)(0) = 2.6*10^{-6}$,
P2: $n_e(0) = 3*10^{13}$ cm^{-3}, $(n_o/n_e)(0) = 1.3*10^{-6}$,
P3: $n_e(0) = 6*10^{13}$ cm^{-3}, $(n_o/n_e)(0) = 2.6*10^{-6}$,
P4: $n_e(0) = 6*10^{13}$ cm^{-3}, $(n_o/n_e)(0) = 1.3*10^{-6}$.

The assumed neutral beam is characterized by the following items:

Beam energy components: E_o, $E_o/2$, $E_o/3$
Particle current into the torus: $I_o = I_1 + I_2 + I_2$
Neutral power into the torus: $P_o = P(E_o)+P(E_o/2)+P(E_o/3)$

Half of the power is delivered by co-injection and counter-injection, respectively. Calculations were done for beam energies with E_o = 30 keV, 40 keV, 50 keV and 60 keV. Two different neutral beam compositions were considered:

N1: $I_1 = 2*I_2 = 2*I_2$; $(P(E_o) = 4*P(E_o/2) = 6*P(E_o/3))$,
N2: $I_1 = I_2 = 0.67*I_2$; $(P(E_o) = 2*P(E_o/2) = 2*P(E_o/3))$.

All the results in this section refer to an injection geometry characterized by R_c = 144 cm and R_s = 15 cm (see fig. 1).

V.2 RESULTS

The relative particle losses ($\Delta I/I_o$), the relative power losses ($\Delta P/P_o$) and the increase of Z_{eff} (ΔZ_{eff}) are illustrated in fig. 14 as functions of the extraction voltage (U_o), assuming the neutral beam composition N1 ($I_1 = 2*I_2 = 2*I_3$). The contributions of the basic processes during beam absorption (A1: absorption and confinement, A2: absorption by CX) and particle slowing down (B1: CX during slowing-down, B2: scattering into the loss region) are plotted in the case of plasma parameter set P1. Finite reionization of neutrals, as described above, was taken into account for A2 and B1.

The particle losses are relatively high (55 - 75 %). Doubling the neutral background density leads to an increase of $\Delta I/I_o$ of about 10 %. These results indicate that neutral injection is not a very suitable method of particle refuelling. As stated above, however, the calculated particle losses represent a lower limit

for the actual "refuelling efficiency". Since the CX processes during slowing-down (B1) considerably contribute to $\Delta I/I_o$, a more exact treatment of the ion balance will probably change the results in a more positive direction.

The power transfer to the plasma is evidently more effective. More than 70 % of the injected power is delivered to the plasma particles. This is in qualitative agreement with experimental results where effective heating with a small density increase was obtained /13/.

The impurity increase was determined by

$$\Delta Z_{eff} = \frac{\Delta n_I}{n_e} Z_I \, (Z_I - Z_{eff}) \, .$$

Δn_I, the increase in impurity concentration, may be obtained from the impurity influx calculated in the way mentioned above. It was further assumed that the heavy impurities are ionized to $Z_I = 25$, that their confinement time is of the order of the particle confinement time $\tau_I = 50$ ms, and that a total power of $P_o = 3$ MW is injected into the torus. For low plasma densities and low injection energies ΔZ_{eff} may not be regarded as a negligible quantity.

The assumed neutral beam composition N1 requires an extracted ion beam with a high content of H^+ ions (about 80 % at $U_o = 50$ kV). Results on the basis of beam composition N2 (H^+ content at $U_o = 50$ kV: $\simeq$ 65 %) with reference to parameter set P1 are given in fig. 15. A small increase in power transfer can be observed compared with assumption N1 ($\simeq$ 2 %), but the overall change is not very significant.

Figure 16 shows a comparison of the results for plasma parameter set P1 and neutral beam composition N2, assuming two different basic conditions:

(a) the power injected into the torus is fixed, P_o = 3 MW, irrespective of U_o;
(b) the current extracted from the ion sources is fixed, $I_{I.S.}$ = 4*40 A for all extraction voltages.

Case (b) corresponds to the high-voltage facilities which will be available for the injection experiment. This assumption requires an estimation of all power losses in the beam line system due to neutralization efficiency and reionization in order to obtain the power transferred into the torus. Such calculations were done using a program developed at IPP /14/.

Condition (a) (left-hand side in fig. 16) leads to a power absorbed by the plasma which is nearly independent of U_o. The variation is less than 5 %, a small minimum occuring at 50 kV. Again, ΔZ_{eff} becomes relatively high with decreasing extraction voltage ($\Delta Z_{eff} \simeq 1.7$ at U_o = = 30 kV). This is partly due to the high neutral beam current necessary to attain the high neutral power of 3 MW.

Condition (b) (right-hand side in fig. 16) results in increasing absorbed power with higher extraction voltage, corresponding to the increasing power extracted from the ion sources. Ion heating as well as the absorbed and thermalized particle current is nearly independent of the beam energy. Although the number of extracted particles is assumed to be constant, they cause a strongly energy dependent impurity increase, mainly determined

by the CX cross-section for beam absorption. If case (b) is accepted as an experimental boundary condition, power transfer and impurity increase call for the highest possible extraction voltage.

V.3 PLANNED EXPERIMENTAL INJECTION PARAMETERS

One of the main purposes of the considerations outlined was to obtain criteria for determining the injection parameters in ASDEX. It is intended to provide additional heating power to the plasma which well exceeds the ohmic heating. Furthermore, it should be possible to deposit this power mainly in the plasma centre. The impurity increase connected directly with the heating process should be kept as small as possible. Since ASDEX is a divertor experiment requiring refuelling, the particle current added to the plasma is a further criterion for the choice of the parameters.

The calculations have shown that the power transferred to the plasma is not very sensitive to the extraction voltage. Injection energies below 40 keV, however, result in preferential particle deposition in the outer plasma region (see fig. 5) and, consequently, in increasing plasma-wall interaction. Furthermore, beam absorption at low particle energies is mainly due to CX processes providing the strong increase in ΔZ_{eff}, mentioned above. An extraction voltage of 40 kV is therefore considered as a lower limit for the injection system. The upper limit is partly given by the absorption probability at low plasma densities ($E_o \lesssim 60$ keV, fig. 5); the main restriction, however, are of technological origin.

Since particle refuelling is nearly independent of the injection energy, it was decided to provide experimentally for an extraction voltage U_o between 40 and 50 kV. Together with an extracted ion current of 40 A for each of the four ion sources, this should lead to the following results (see fig. 16):

- Power absorbed within the plasma: $P_o \simeq 2.5$ MW
- Particle current added to the plasma: $I_o \gtrsim 30 - 35$ A
- Impurity increase: $\Delta Z_{eff} \simeq 1.0 - 1.5$

This values certainly allow one to study a plasma which is predominantly determined by non-ohmic heating.

An additional parameter which strongly affects the injection system design is given by the pulse duration of the neutral beam. In order to investigate quasi-stationary plasma conditions, the pulse duration should be several times as long as the expected energy confinement time ($\tau_E \simeq 50 - 100$ ms). Values of $\tau_{pulse} \gtrsim 0.2$ s (0.2 - 1.0 s) are therefore aimed at for the injection experiment.

VI PROFILE SHAPING

By changing the injection geometry different radial particle deposition (fig. 3) and hence different heating power deposition profiles will be obtained. In principle, this could be a method of controlling the electron temperature profiles and, as a consequence, of shaping the plasma current profile. It has been suggested that internal disruptions may be suppressed by preferentially depositing the neutral beam near the plasma boundary /15/.

The following calculations deal with the possibility of modifying the heating power profiles for ions and electrons by varying R_c, the distance between the torus centre and the beam axis (see fig. 1). Experimentally, this may be achieved by pivoting the injection system. Detailed predictions of the effects on plasma profiles, however, require selfconsistent allowance for the heating rates in an appropriate simulation code. Such calculations have not been done until now.

The heating power density profile for plasma ions and electrons may be written in accordance with eq. (III.5) (see also ref. /7/):

$$P_I\ (r) = (I_o * U_o\ /\ V_{pl}) * H(r) * G_I(r),$$
$$P_e\ (r) = (I_o * U_o\ /\ V_{pl}) * H(r) * G_e(r).$$

Some results are illustrated in fig. 17. For calculating $G_I(r)$ and $G_e(r)$ CX losses of the fast ions were taken into account, assuming the (n_o/n_e) profile described in Section V ($(n_o/n_e)\ (0) = 2.6 * 10^{-6}$).

Pronounced variation of heating power profiles may be obtained only by injecting the neutral beam with a relatively high R_c value, i.e. by depositing the fast ions preferentially in the outer plasma region. Higher R_c values, however, are connected with decreasing beam absorption and increasing particle losses, mainly owing to the higher neutral background density near the plasma boundary. Power transfer to the plasma will therefore be reduced and the impurity influx will increase. Furthermore, a plasma heated near the boundary will give rise to enhanced plasma-wall interaction. Calculations, similar to those in Section V, for E_o = 50 keV

and plasma parameter sets P1 and P3 have indicated that an additional 10 % of the injected particles and power will be lost, being accompanied by an additional impurity influx of about 10 %, if R_c = 170 cm is taken instead of R_c = 144 cm.

In order to study experimentally the influences of different fast ion depositions on the various plasma profiles, it is intended to provide the possibility of pivoting the injection system.

VII SUMMARY

The considerations outlined were performed in order to determine the injection parameters required for the neutral injection experiment on the ASDEX tokamak. Special emphasis has been placed on the energy dependence of the various effects which determine the efficiency of power transfer to the plasma ions and electrons, the particle refuelling and the increase of the impurity level. The parameters envisaged, as quoted in Section V, should allow study of a plasma which is predominantly determined by non-ohmic heating, producing only a tolerable impurity increase.

So far, the calculations have not taken into account the variations of plasma parameters or profiles during the neutral beam pulse. Variation of density, temperature and impurity concentration will cause changes in the beam deposition and heating power profiles. It will therefore be necessary to incorporate neutral beam heating into an adequate plasma simulation code in order to describe beam absorption and fast ion slowing-down more exactly and to get detailed information on the response of the plasma to the neutral beam.

Furthermore, no attention has yet been paid to the existence of the divertor in the ASDEX tokamak. The losses of fast charged particles due to non-confined orbits may be influenced by the presence of the separatrix and the impurity influx connected with these losses may be suppressed when these fast ions are guided into the divertor chambers. Knowledge of fast ion drift surfaces in the complete magnetic field configuration is required to calculate these effects. However, since the losses of fast ions on non-confined orbits are usually small, no significant variation of the results may be expected. In an unload divertor experiment (the ASDEX divertor will be of the unload-type) the neutral particle density is reduced /16/. Although the actual neutral particle density will also depend on the refuelling method employed, the (n_o/n_e) values presumed in the above calculation may be too pessimistic, i.e. the losses during particle slowing-down and the associated impurity influx may be overestimated. These qualitative arguments show that the influence of the divertor on the processes considered here - if there is any significant influence - will change the results in a favourable direction.

The author wishes to acknowledge many valuable discussions during this work with Drs. E. Speth, W. Ott and J.H. Feist from the neutral injection group and Drs. M. Keilhacker and G. Haas from the ASDEX team.

REFERENCES

/1/ R. Allgeyer et al., Proc. 6th Symp. Engin. Probl. in Fusion Research, San Diego, 1975, p. 378

/2/ G. Haas et al., 3rd Symp. on Plasma Heating in Toroidal Devices, Varenna, 1976, p. 308

/3/ J.A. Rome, J.D. Callen, J.F. Clarke, Nuclear Fusion 14 (1974) 141

/4/ T.H. Stix, Plasma Physics 14 (1971) 367

/5/ P. Moriette, 7th Yugoslav. Symp. on Phs. of Ionized Gases, Rovinj, 1974, p. 43

/6/ S. Rehker, E. Speth, Lab. Rep. IPP 2/217 (1974)

/7/ W. Ott et al., Lab. Rep. IPP, in preparation

/8/ A.C. Riviere, Nuclear Fusion 11 (1971) 363

/9/ L. A. Berry et al., 5th Int. Conf. on Plasma Physics and Controlled Nuclear Fusion, Tokyo, 1974, Vol. 1, p. 101

/10/ J.A. Rome et al., Nuclear Fusion 16 (1976) 55

/11/ B.M.U. Scherzer, J. Vac. Sci. Technol. 13 (1976) 420

/12/ D.F. Düchs, private communication

/13/ TFR-Group, 3rd Intern. Meeting on Theoret. and Experim. Aspects of Heating of Toroidal Plasmas, Grenoble 1976, Vol. 2, p. 141

/14/ J.H. Feist, Lab. Rep. IPP, in preparation

/15/ A. Nicolai, Proc. Internat. Symp. on Plasma Wall Interaction, Jülich, 1976, in press

/16/ M. Keilhacker, Lab. Rep. IPP III/33 (1976)

FIGURE CAPTIONS

Fig. 1 Schematic drawing of the injection geometry.

Fig. 2 Mean free path (λ_o) as function of neutral particle energy (E_o) at various peak densities ($n_e(o)$) with Z_{eff} as parameter.

Fig. 3 Fast ion deposition profiles for co- and counter--injection. Fixed values: R_s = 15 cm, x_s = 2.6 cm, parameters: a/λ_o and R_c. Numbers in parentheses: amount of the injected beam absorbed and confined within the plasma

Fig. 4 Relative losses due to incomplete absorption and confinement as function of a/λ_o.

Fig. 5 Lines of a/λ_o = const in the ($n_e(o)$ - E_o) plane.

Fig. 6 Relative particle losses and relative energy losses as function of (n_o/n_e).

Fig. 7 Energy transfer to ions and electrons as function of (E_o/E_c) for several (n_o/n_e) values.

Fig. 8 Loss regions for protons in ASDEX. r_b: birth radius of the fast ions (at $\theta = 0^o$).

Fig. 9 $L_{LR}(r)$, the amount of the neutral beam being absorbed between r and the plasma boundary for co- and counter-injection.

Fig. 10 Probability of neutral beam absorption by CX on plasma ions as function of beam energy E_o with Z_{eff} as parameter.

Fig. 11 Impurity influx caused by the various processes (see text) as function of beam energy E_o.

Fig. 12 Mean reionization probability as function of the mean plasma density n_e.

Fig. 13 Profiles for T_e and (n_o/n_e) used in the following calculations.

Fig. 14 Particle losses, energy losses and impurity increase as function of the extraction voltage U_o. Assumed beam composition: N1: $I_1 = 2 \times I_2 = 2 \times I_3$.
P1, P2, P3, P4: various plasma parameters (see text).
A1: beam absorption and confinement, A2: absorption by CX, B1: CX during slowing-down, B2: scattering into the loss region.

Fig. 15 Particle losses, energy losses and impurity increase as function of the extraction voltage U_o. Assumed beam composition. N2: $I_1 = I_2 = 0.67\ I_3$.
Further abbreviations: see Fig. 14.

Fig. 16 Comparison of the results for constant power injected into the torus (left-hand side) and constant current extracted from the ion sources (right-hand side). Assumed plasma parameters: P1: assumed beam composition. N2 (see text).

Fig. 17 Different heating power profiles for electrons and ions obtained by changing the injection geometry (R_c).

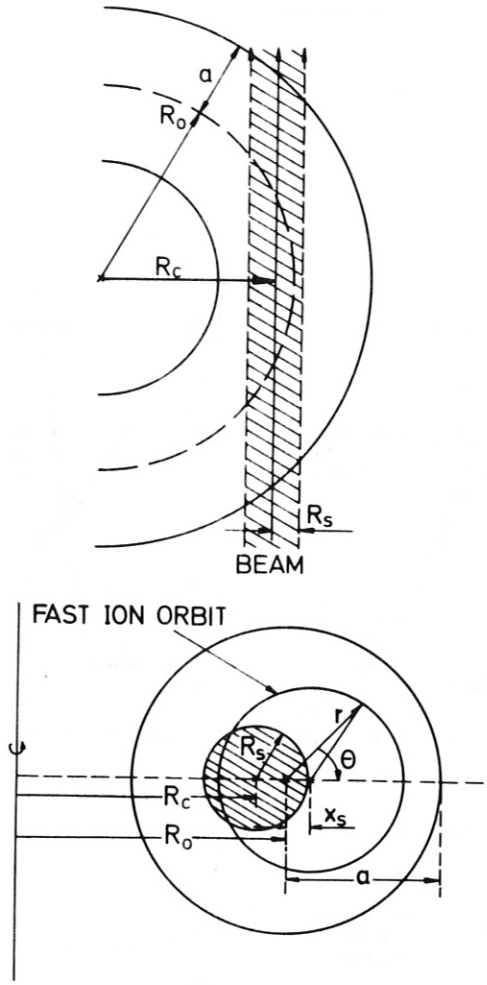
a
R_o
R_c
R_s
BEAM
FAST ION ORBIT
r
θ
R_s
R_c
R_o
x_s
a

Fig. 1

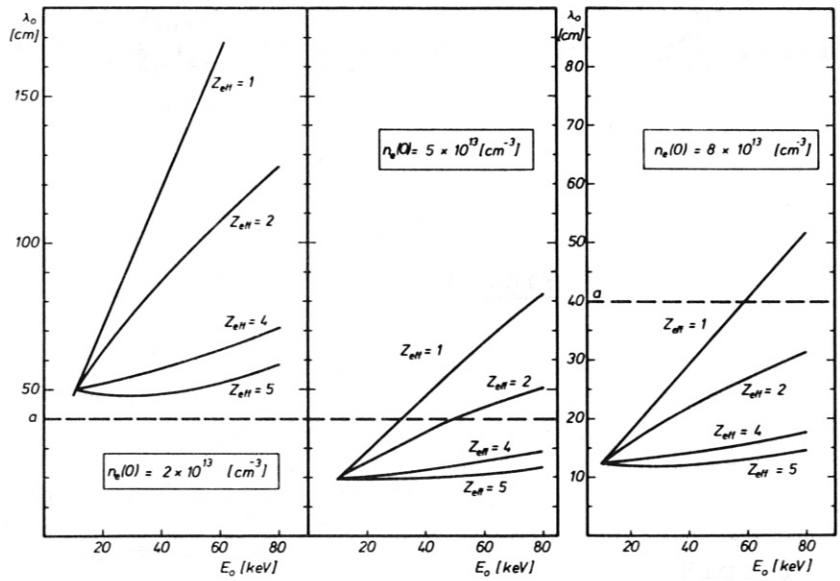
λ_o [cm]
150
100
50
a
Z_{eff} = 1
Z_{eff} = 2
Z_{eff} = 4
Z_{eff} = 5
$n_e(0)$ = 2 × 10^{13} [cm^{-3}]
$n_e(0)$ = 5 × 10^{13} [cm^{-3}]
$n_e(0)$ = 8 × 10^{13} [cm^{-3}]
80
70
60
50
40
30
20
10
20
40
60
80
E_o [keV]

Fig. 2

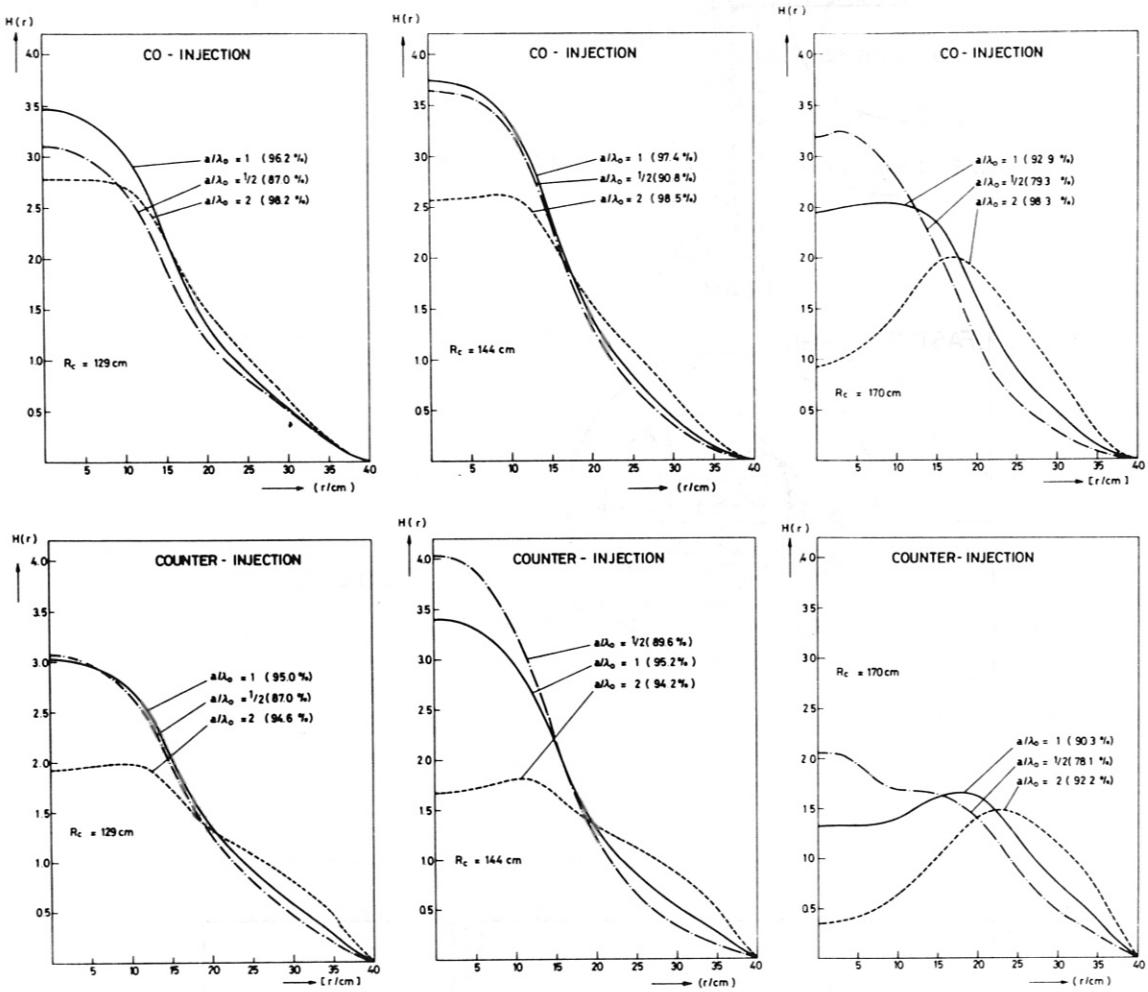
H(r)
CO - INJECTION
a/λ₀ = 1 (96.2 %)
a/λ₀ = 1/2 (87.0 %)
a/λ₀ = 2 (98.2 %)
Rc = 129 cm
(r/cm)
CO - INJECTION
a/λ₀ = 1 (97.4 %)
a/λ₀ = 1/2 (90.8 %)
a/λ₀ = 2 (98.5 %)
Rc = 144 cm
(r/cm)
CO - INJECTION
a/λ₀ = 1 (92.9 %)
a/λ₀ = 1/2 (79.3 %)
a/λ₀ = 2 (98.3 %)
Rc = 170 cm
[r/cm]
COUNTER - INJECTION
a/λ₀ = 1 (95.0 %)
a/λ₀ = 1/2 (87.0 %)
a/λ₀ = 2 (94.6 %)
Rc = 129 cm
[r/cm]
COUNTER - INJECTION
a/λ₀ = 1/2 (89.6 %)
a/λ₀ = 1 (95.2 %)
a/λ₀ = 2 (94.2 %)
Rc = 144 cm
(r/cm)
COUNTER - INJECTION
Rc = 170 cm
a/λ₀ = 1 (90.3 %)
a/λ₀ = 1/2 (78.1 %)
a/λ₀ = 2 (92.2 %)
(r/cm)

Fig. 3

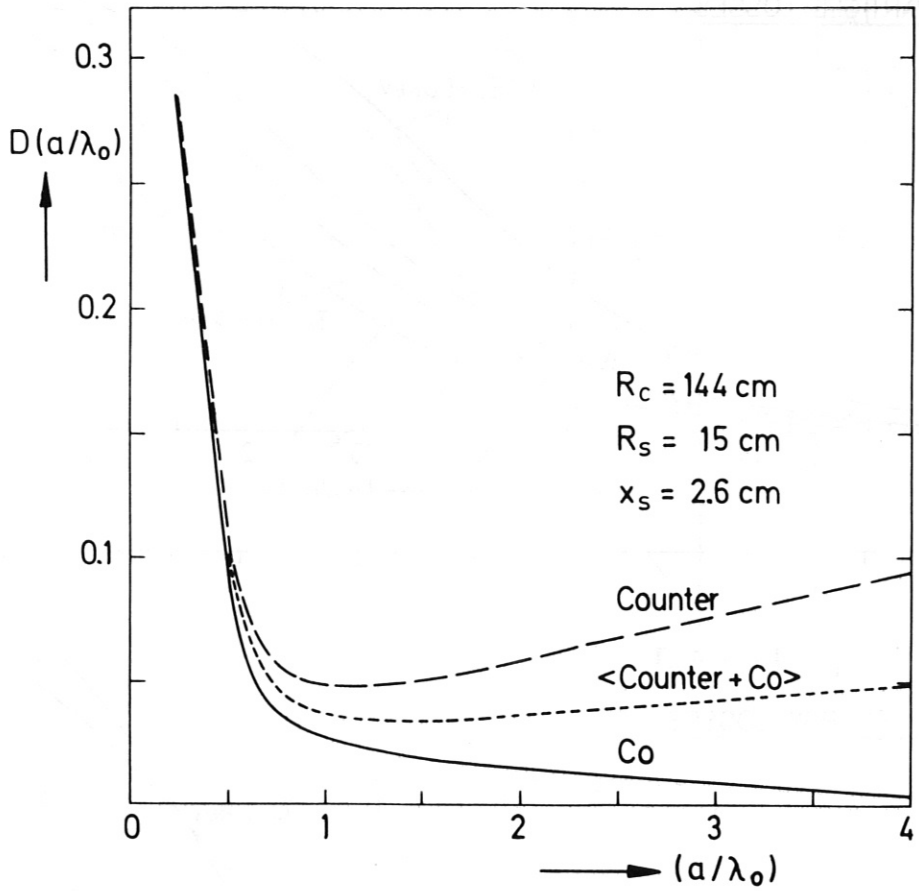
0.3
0.2
0.1
D(a/λo)
Rc = 144 cm
Rs = 15 cm
xs = 2.6 cm
Counter
<Counter + Co>
Co
0
1
2
3
4
(a/λo)

Fig. 4

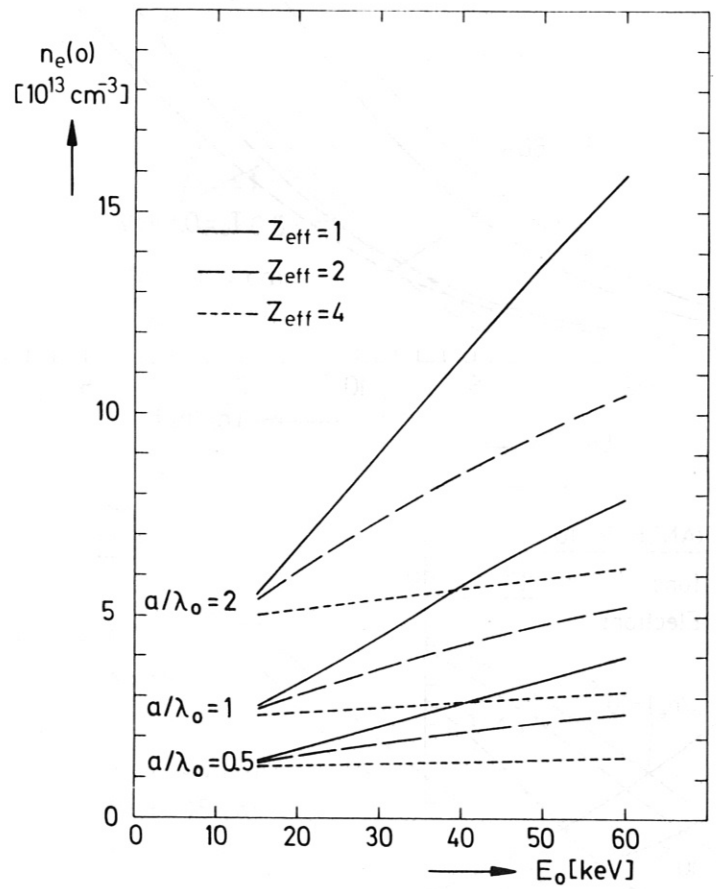
ne(o)
[10^13 cm^-3]
15
10
5
0
Zeff = 1
Zeff = 2
Zeff = 4
a/λo = 2
a/λo = 1
a/λo = 0.5
0
10
20
30
40
50
60
Eo[keV]

Fig. 5

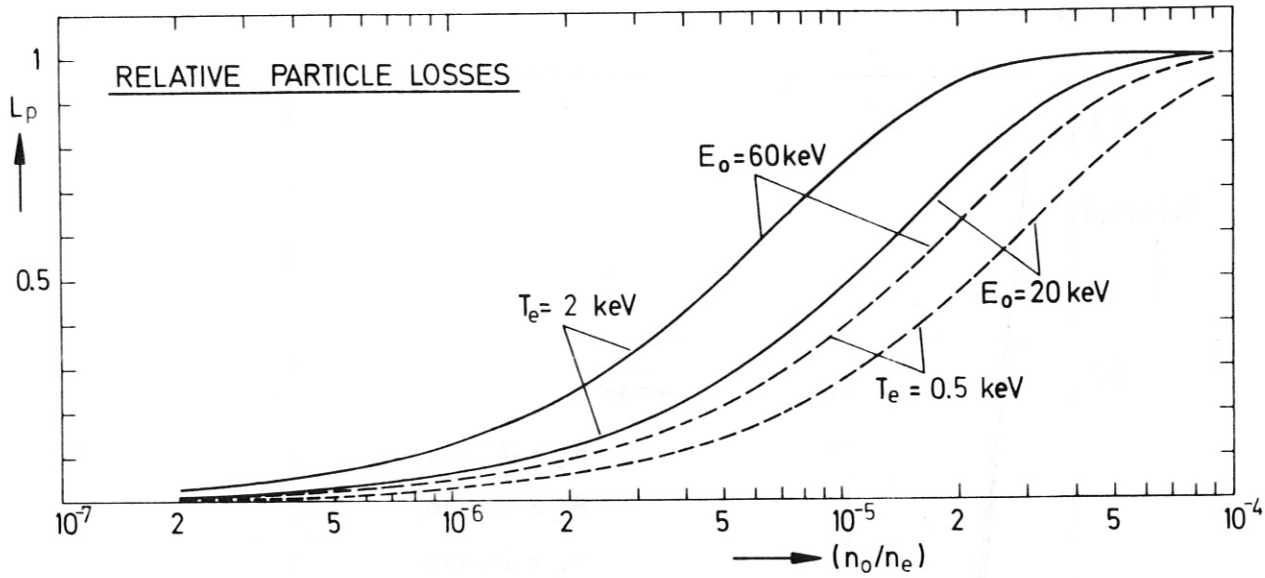
RELATIVE PARTICLE LOSSES
L_p
1
0.5
E_o=60keV
E_o=20 keV
T_e= 2 keV
T_e = 0.5 keV
10^{-7}
2
5
10^{-6}
2
5
10^{-5}
2
5
10^{-4}
(n_o/n_e)

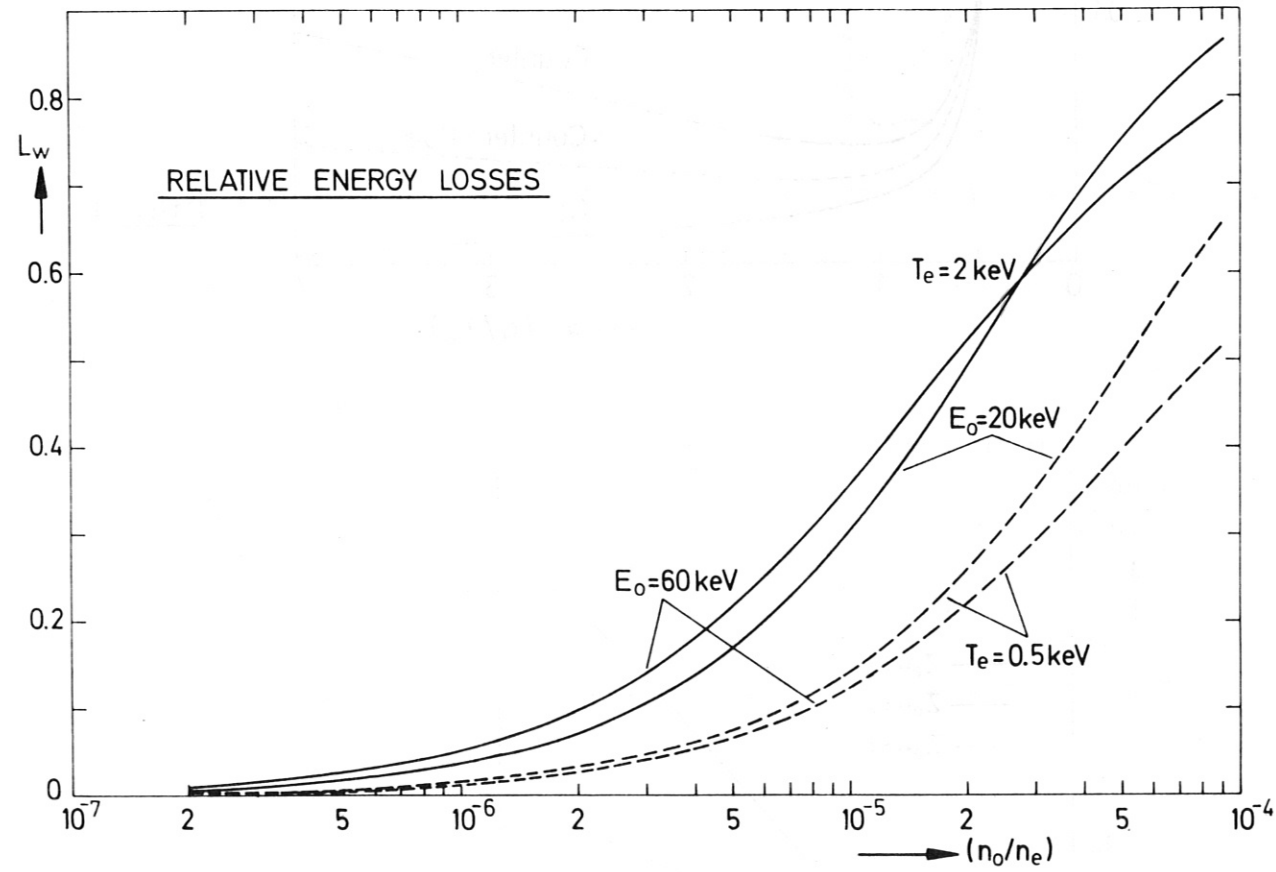
RELATIVE ENERGY LOSSES
L_w
0.8
0.6
0.4
0.2
0
T_e=2 keV
E_o=20keV
E_o=60 keV
T_e=0.5keV
10^{-7}
2
5
10^{-6}
2
5
10^{-5}
2
5
10^{-4}
(n_o/n_e)

Fig. 6

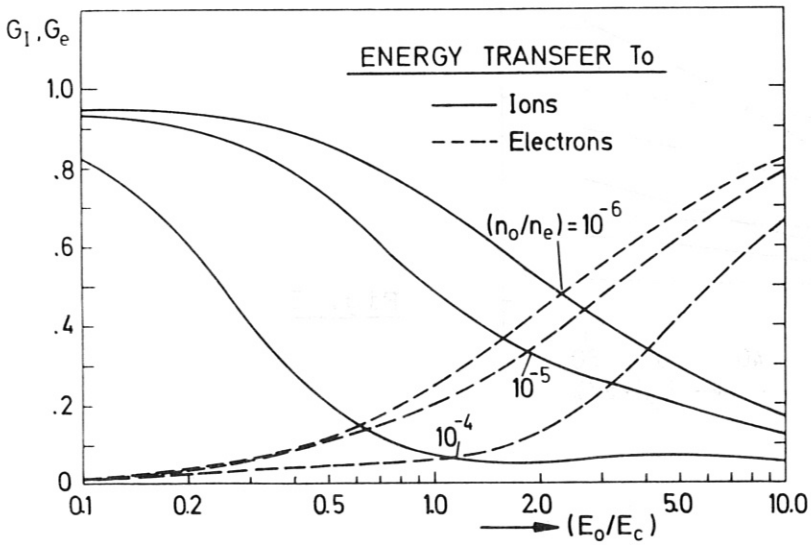
G_I, G_e
ENERGY TRANSFER To
Ions
Electrons
1.0
.8
.6
.4
.2
0
$(n_o/n_e) = 10^{-6}$
10^{-5}
10^{-4}
0.1
0.2
0.5
1.0
2.0
5.0
10.0
(E_o/E_c)

Fig. 7

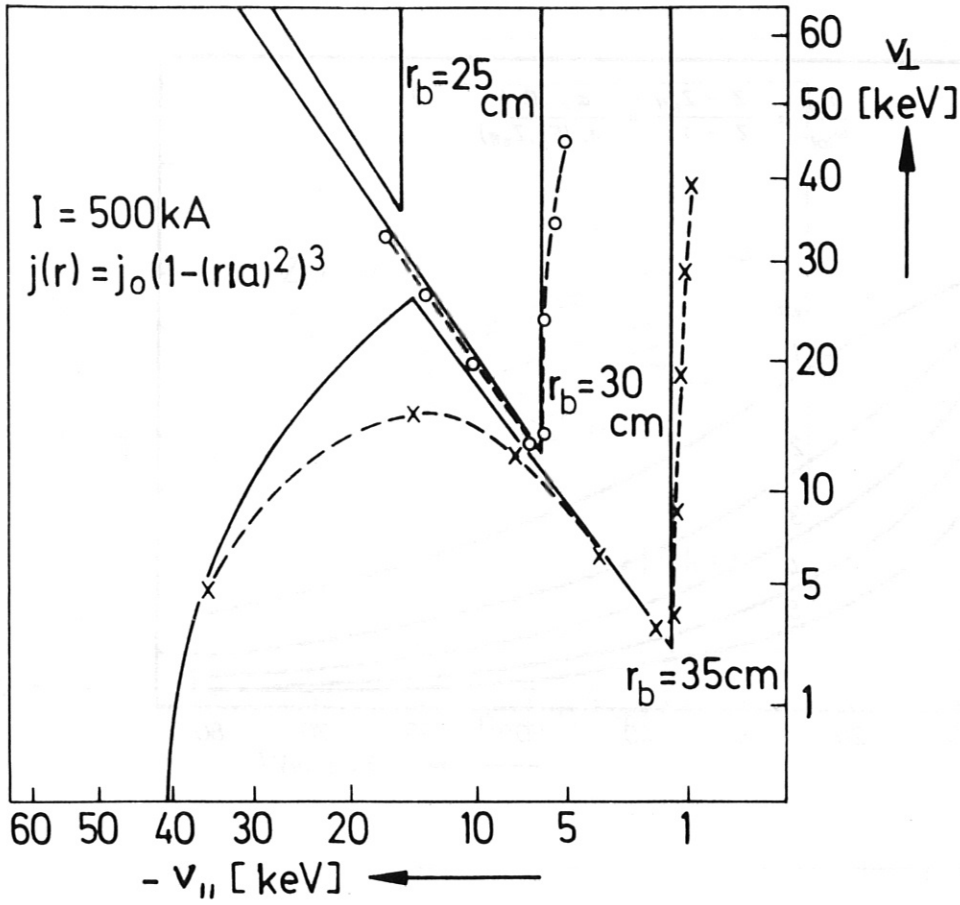
I = 500kA
j(r) = j₀(1-(r/a)²)³
r_b=25 cm
r_b=30 cm
r_b=35cm
v⊥ [keV]
60
50
40
30
20
10
5
1
60 50 40 30 20 10 5 1
- v∥ [keV]

Fig. 8

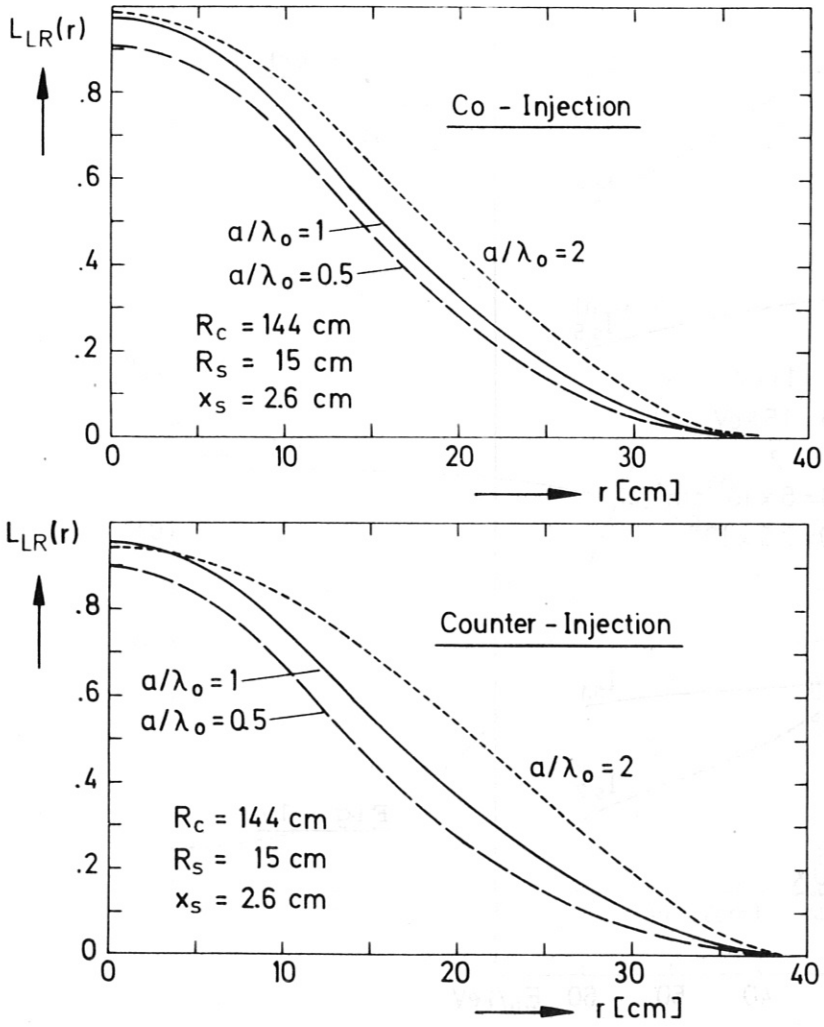
L_LR(r)
Co - Injection
a/λ₀ = 1
a/λ₀ = 0.5
a/λ₀ = 2
R_c = 144 cm
R_s = 15 cm
x_s = 2.6 cm
r [cm]
Counter - Injection
a/λ₀ = 1
a/λ₀ = 0.5
a/λ₀ = 2
R_c = 144 cm
R_s = 15 cm
x_s = 2.6 cm
r [cm]

Fig. 9

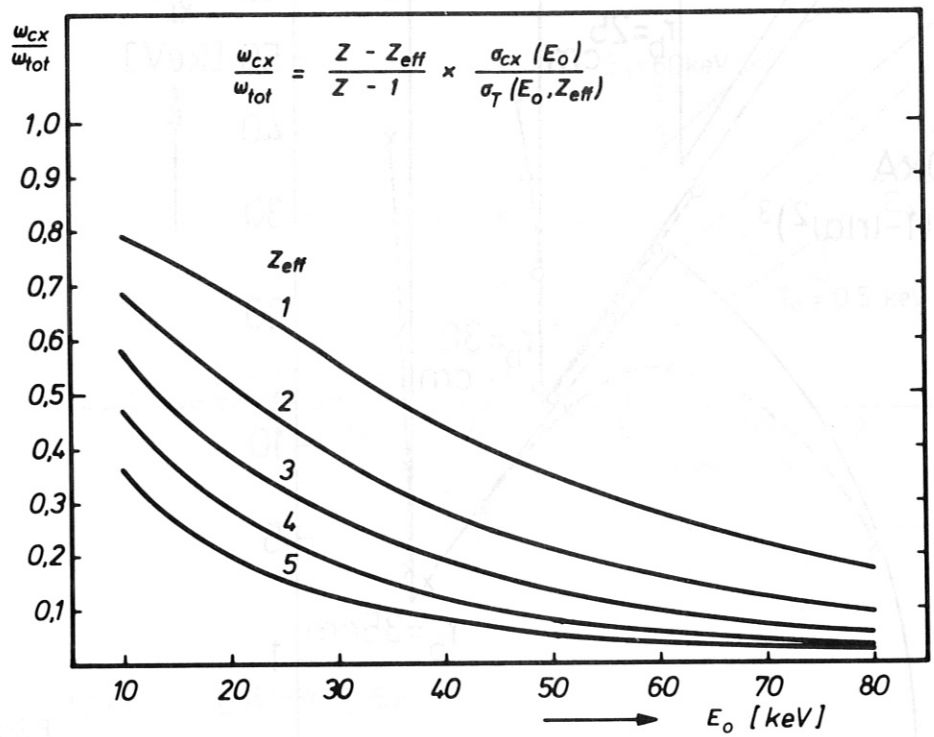
$\frac{\omega_{cx}}{\omega_{tot}} = \frac{Z - Z_{eff}}{Z - 1} \times \frac{\sigma_{cx}(E_o)}{\sigma_T(E_o, Z_{eff})}$
$\frac{\omega_{cx}}{\omega_{tot}}$
1,0
0,9
0,8
0,7
0,6
0,5
0,4
0,3
0,2
0,1
Z_{eff}
1
2
3
4
5
10
20
30
40
50
60
70
80
E_o [keV]

Fig. 10

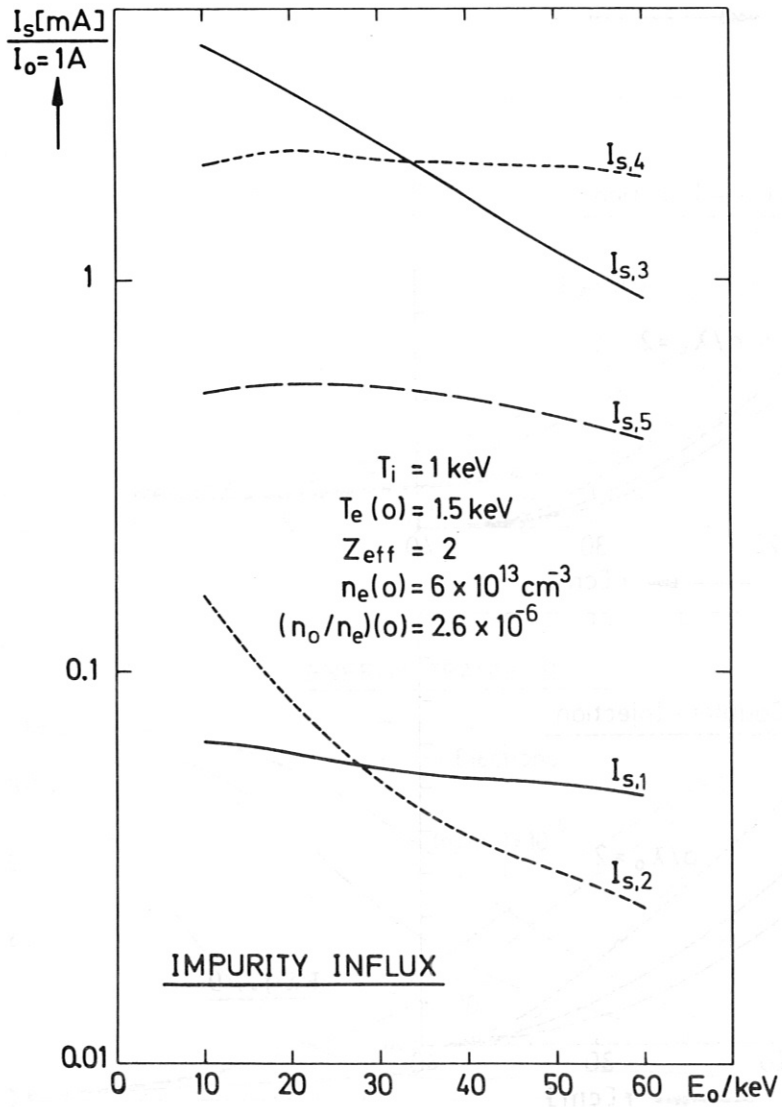
$\frac{I_s[mA]}{I_o = 1A}$
1
0.1
0.01
$I_{s,4}$
$I_{s,3}$
$I_{s,5}$
T_i = 1 keV
$T_e(o)$ = 1.5 keV
Z_{eff} = 2
$n_e(o) = 6 \times 10^{13} cm^{-3}$
$(n_o/n_e)(o) = 2.6 \times 10^{-6}$
$I_{s,1}$
$I_{s,2}$
IMPURITY INFLUX
0
10
20
30
40
50
60
E_o/keV

Fig. 11

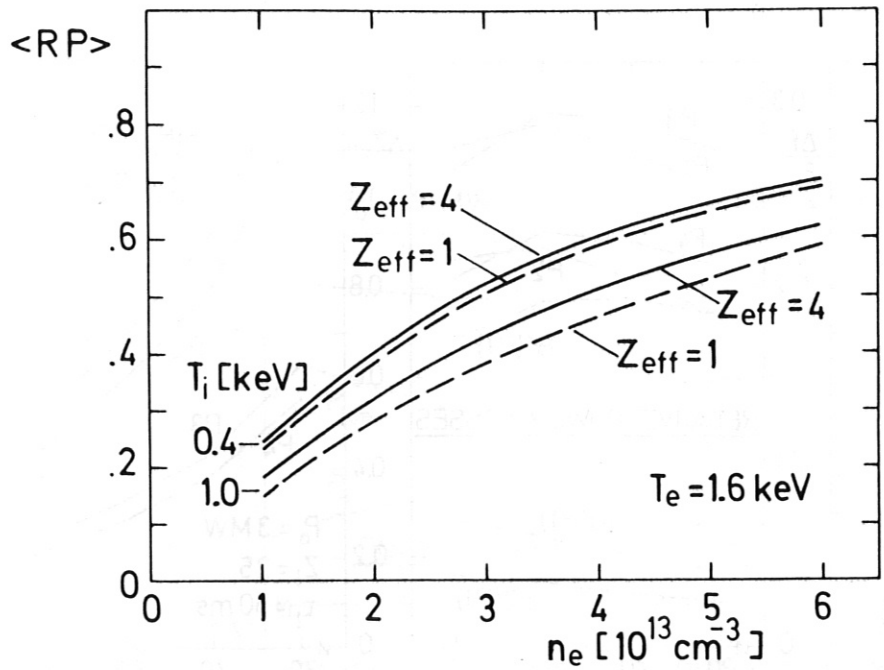
<RP>
.8
.6
.4
.2
0
Zeff = 4
Zeff = 1
Zeff = 4
Zeff = 1
Ti [keV]
0.4
1.0
Te = 1.6 keV
0
1
2
3
4
5
6
ne [10^13 cm^-3]

Fig. 12

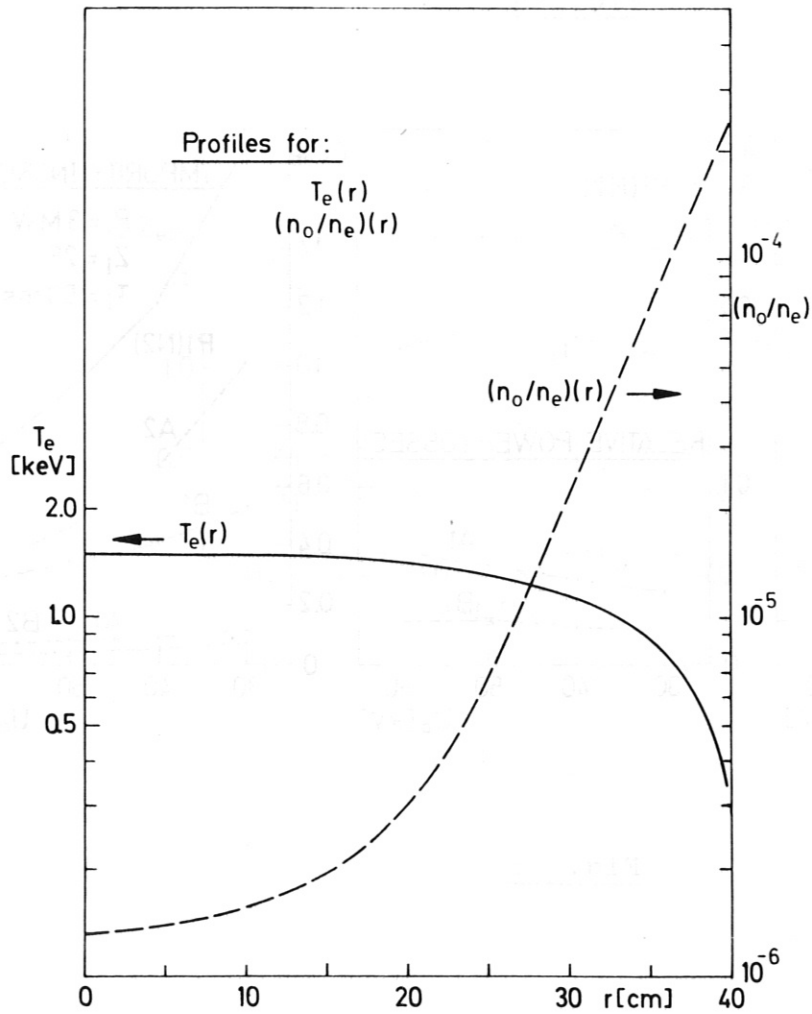
Profiles for:
Te(r)
(no/ne)(r)
10^-4
(no/ne)
(no/ne)(r)
Te
[keV]
2.0
Te(r)
1.0
10^-5
0.5
10^-6
0
10
20
30
r[cm]
40

Fig. 13

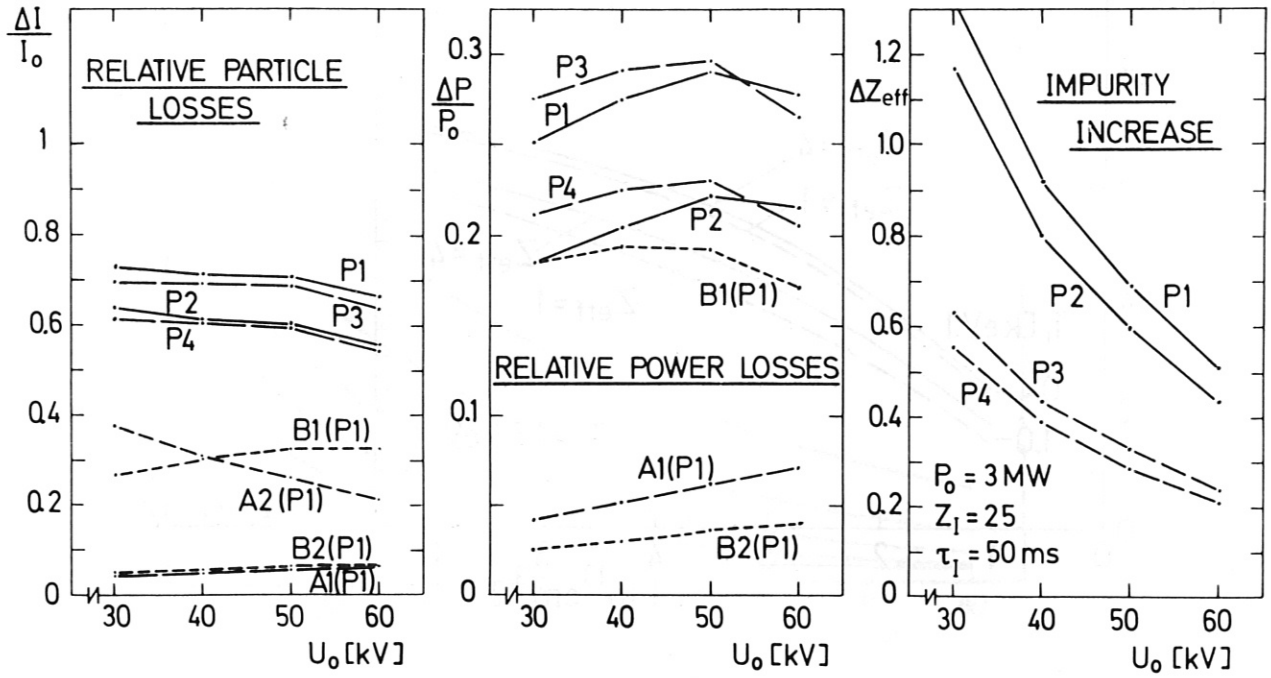
ΔI/I₀
RELATIVE PARTICLE LOSSES
P1
P2
P3
P4
B1(P1)
A2(P1)
B2(P1)
A1(P1)
U₀ [kV]
ΔP/P₀
P3
P1
P4
P2
B1(P1)
RELATIVE POWER LOSSES
A1(P1)
B2(P1)
U₀ [kV]
ΔZeff
IMPURITY INCREASE
P2
P1
P3
P4
P₀ = 3 MW
Z_I = 25
τ_I = 50 ms
U₀ [kV]

Fig. 14

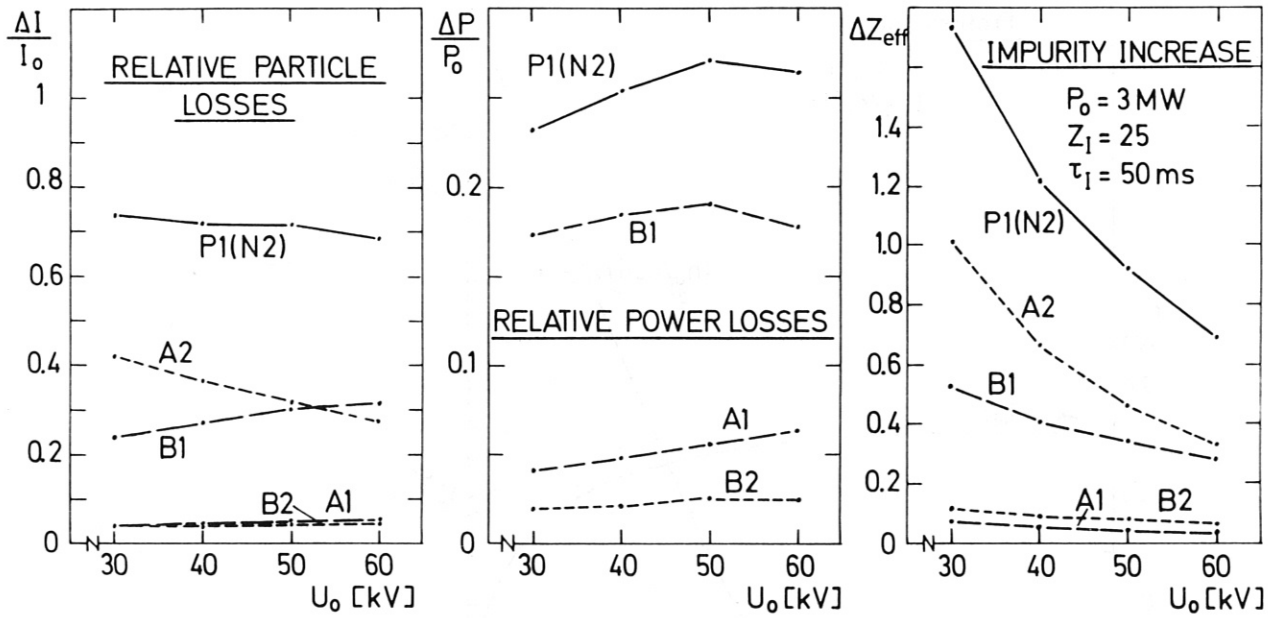
ΔI/I₀
RELATIVE PARTICLE LOSSES
P1(N2)
A2
B1
B2
A1
U₀ [kV]
ΔP/P₀
P1(N2)
B1
RELATIVE POWER LOSSES
A1
B2
U₀ [kV]
ΔZeff
IMPURITY INCREASE
P₀ = 3 MW
Z_I = 25
τ_I = 50 ms
P1(N2)
A2
B1
A1
B2
U₀ [kV]

Fig. 15

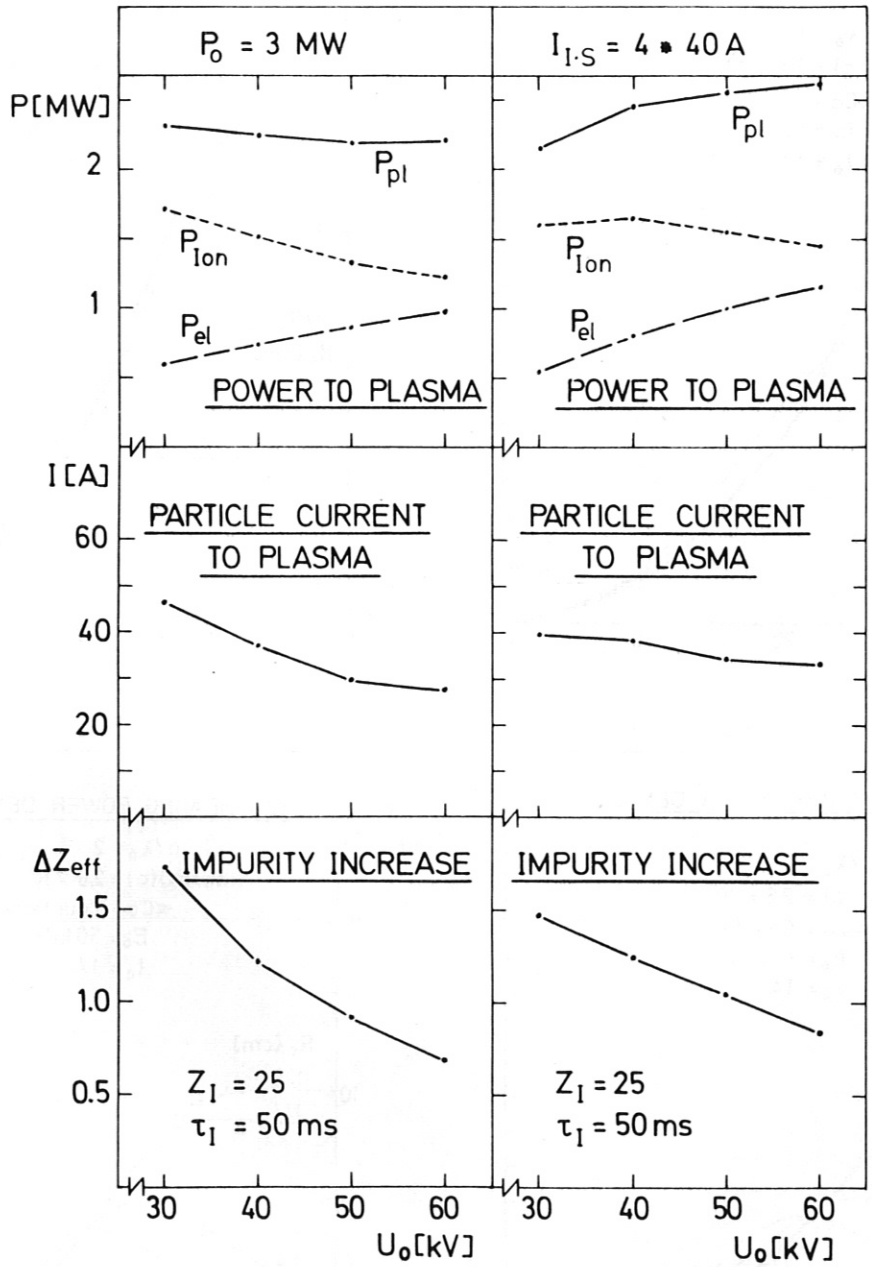
P₀ = 3 MW
I_I·S = 4 • 40 A
P[MW]
2
1
P_pl
P_Ion
P_el
POWER TO PLASMA
I [A]
60
40
20
PARTICLE CURRENT TO PLASMA
ΔZ_eff
1.5
1.0
0.5
IMPURITY INCREASE
Z_I = 25
τ_I = 50 ms
30
40
50
60
U₀[kV]

Fig. 16

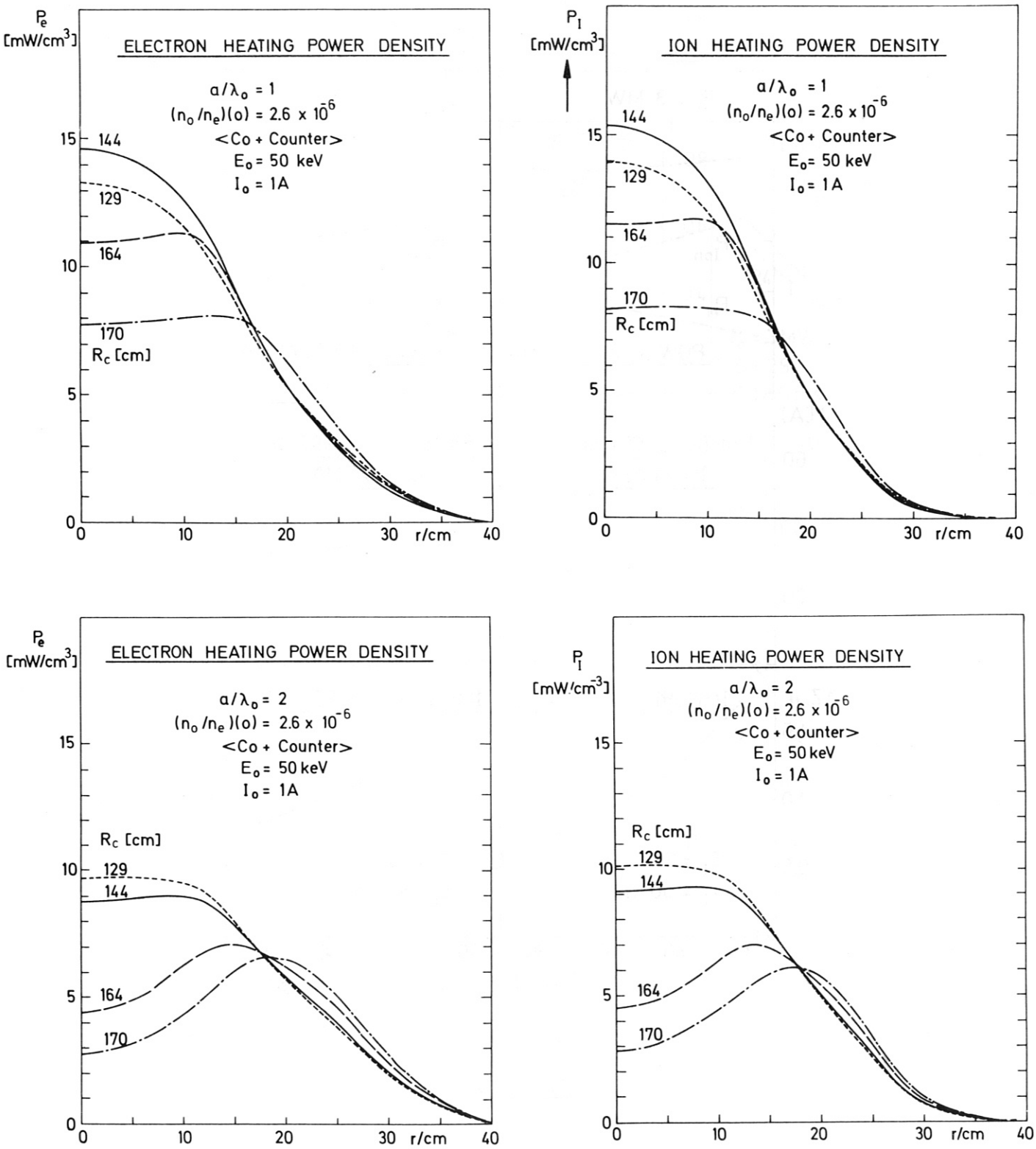
P_e [mW/cm^3]
ELECTRON HEATING POWER DENSITY
$a/\lambda_o = 1$
$(n_o/n_e)(o) = 2.6 \times 10^{-6}$
<Co + Counter>
$E_o = 50$ keV
$I_o = 1A$
144
129
164
170
R_c [cm]
r/cm
P_I [mW/cm^3]
ION HEATING POWER DENSITY
$a/\lambda_o = 1$
$(n_o/n_e)(o) = 2.6 \times 10^{-6}$
<Co + Counter>
$E_o = 50$ keV
$I_o = 1A$
144
129
164
170
R_c [cm]
r/cm
P_e [mW/cm^3]
ELECTRON HEATING POWER DENSITY
$a/\lambda_o = 2$
$(n_o/n_e)(o) = 2.6 \times 10^{-6}$
<Co + Counter>
$E_o = 50$ keV
$I_o = 1A$
R_c [cm]
129
144
164
170
r/cm
P_I [mW/cm^3]
ION HEATING POWER DENSITY
$a/\lambda_o = 2$
$(n_o/n_e)(o) = 2.6 \times 10^{-6}$
<Co + Counter>
$E_o = 50$ keV
$I_o = 1A$
R_c [cm]
129
144
164
170
r/cm

Fig. 17